The Numerical Aerodynamic Investigation of Swirling Inlet flow in a Vaporizer Tube Micro-Gas Turbine Combustor

Bronwyn C Meyers and Jan-Hendrik Grobler
bmeyers@csir.co.za or meyers.bronwyn@gmail.com
The Council for Scientific and Industrial Research
Aeronautic Systems Impact Area
Pretoria
South Africa

Glen C Snedden
University of KwaZulu Natal
School of Mechanical Engineering
Durban
South Africa

ABSTRACT

A combustor was designed for a 200N micro-gas turbine for the model aircraft industry using the NREC design method. Multiple designs resulted which varied in terms of annular area split configuration, hole area splits and relative hole positions. In a previous study two likely preferable designs were selected using a devised scoring method.

For this study, the effect of inlet (diffuser outlet) swirl on the internal aerodynamics of the two combustor designs previously chosen was investigated using a RANS CFD analysis. For each of the two designs a set of varying flow angles was applied at the inlet to the simulation domain. The effect on the establishment of the primary zone features is of specific interest; however, the effects and consequences of the swirl throughout the combustor were investigated.

Some of the results such as mass flow splits and pressure drop are already quantitative in nature, however, the evaluation of the quality of the recirculation zone, mixing and outlet plane flow are of a more qualitative nature.

A scoring system was previously devised in order to apply a quantitative value to the qualitative aspects of the flow, such as Recirculation zone (Rz), Outlet and Mixing, which are initially analysed subjectively. For each feature, the designs were subjectively evaluated relative to each other and given a rating/score.

This scoring methodology for ranking different combustor designs proved to be an effective method for evaluating the effect of inlet swirl on the flow features and behaviour of the chosen combustor designs and thus provide an indication of the likely performance changes to be expected. The methodology was able to indicate which of the two top designs was the better option when considering inlet swirl, however the potential for improvement was revealed when considering scoring in a global context.

This study suggests that for this engine, the inlet swirl could allow for the removal of NGV before the turbine since the flow is fairly well conditioned and “pre-turned” due to the swirling flow progressing to the outlet of the combustor. The removal of the traditional NGV allows for a reduction in NGV pressure losses which compensates for the increased combustor pressure loss experienced due to increased inlet swirl.

Keywords: Combustor; Computational Fluid Dynamics; Evaluation, Inlet Swirl

NOMENCLATURE

alt	Altitude
An	Annulus
C/S	Cross section
CFD	Computational Fluid Dynamics
Dz	Dilution zone
Dzi	Inner dilution zone hole-set
Dzo	Outer dilution zone hole-set
Eff	Efficiency
NGV	nozzle guide vanes
NREC	Northern Research and Engineering Corporation
Pz	Primary zone
Pzi,	Inner primary zone hole-set
Pzo	Outer primary zone hole-set
PzV	Primary hole-set that are vaporiser tubes
RST	Reynolds stress turbulence
Rz	Recirculation zone
SL	Sea Level
SST	Shear Stress Transport
Sz	Secondary zone
Szi	Inner secondary zone hole-set
Szo	Outer secondary zone hole-set
trac	Tracers
Vec	Vectors
Vort	Vortices

Symbols

ΔP	Pressure drop
$\dot{m}$	Mass flow rate
d	Liner diameter
D	Casing Diameter
p	Static pressure
P	Total pressure
T	Temperature
x	Horizontal co-ordinate
x	The fraction of total air required in the outer annulus
y	Vertical co-ordinate
z	Axial co-ordinate

Subscripts

3	Station at the inlet to the combustor
4	Station at the outlet to the combustor
f	Fuel
i	Inner
o	Outer

1.0 INTRODUCTION

A combustor was designed for a 200N micro-gas turbine [1, 2] using the NREC preliminary combustor design method [1, 2, 3]. During the design process, there are various aspects where there are no definitive methodologies for specifying the design detail, such as the design of the hole-sets, and multiple options can be derived that can satisfy the required mass flow split and pressure drop for a particular hole-set.

Hole-set configurations were devised using the process provided in NREC [3] combined with the knowledge that the previous combustor used in the engine had a problem with the inner combustor liner burning away. It was suspected that part of the reason for this was a much lower air flow rate in the inner annulus than the outer annulus due to minimal holes in the inner liner wall. An alternative cause could also be due to annular flow irregularities in the inner annulus such as flow separation [4].

The original combustor design had the vaporizer tubes entering from the outer annulus. In order to approach the combustor development process systematically, it was decided that the first combustors to be developed from the new designs will retain the current vaporizer tube setup with the vaporizer tubes entering from the downstream liner wall fed from the outer annulus.

The first phase of design [1] focussed on correcting the airflow splits between the two annuli and focusing on achieving an improved Primary zone flow pattern that more closely resembles the recirculation in the theory [5, 6]. Multiple preliminary options were designed with a zero-degree inlet swirl condition assumed, and nine preliminary designs were chosen for CFD analysis and evaluation. These designs varied in terms of annular area split configuration, hole area splits and relative hole positions. The evaluation was broken up into the relevant aspects/features, namely, Recirculation zone (Rz), Outlet and Mixing. For each feature, the designs were subjectively evaluated relative to each other and given a rating/score using the method presented in [2]. In this previous study [2] two likely preferable designs were selected using the devised scoring method.

For this study, the effect of inlet (diffuser outlet) swirl on the internal aerodynamics of the previously chosen two combustor designs was investigated using RANS CFD analysis. For each of the two designs a set of varying flow angles (0°, 10°, 20°, 25°, 30°, 33°, 35°, 37° and 40°) was applied at the inlet to the simulation domain. This resulted in 18 different simulations being performed. The effect on the establishment of the primary zone features is of specific interest; however, the effects and consequences of the swirl throughout the combustor were investigated.

It was suspected that, although inlet swirl is potentially detrimental to the combustor aerodynamics, the temperature pattern factor at the outlet as well as causing an increased pressure drop and without necessarily enhancing mixing [6], the swirl could provide some improvement to the previously observed non-ideal outlet flow which demonstrated many multidirectional vortices on the outlet plane which is highly unfavorable for the functioning of the NGV and turbine.

For both designs, the vaporizer tubes are treated as one of the primary zone hole-sets. The major geometrical difference between the two designs was that Design C had the second primary zone hole-set on the outer liner wall in between the vaporizer tubes while Design G had the second primary zone hole-set on the inner liner wall in line with the vaporizer tubes.

The resultant CFD simulation data for the chosen two designs were processed, analysed, and interpreted and the resulting aerodynamic structures were evaluated using the same rating/scoring method as was used when narrowing down the nine designs previously. The combustor/swirl angle simulations with the highest scores overall give an indication of the detrimental or advantageous effect of the inlet swirl.

The results indicate that increasing inlet swirl reduces the generation of vortices throughout the combustor liner with a higher influence in the reduction of the vortices generated on the cross-sectional planes of the combustor. The swirl entering the combustor is increased throughout the length of the combustor and thus a single directional swirling flow is dominant at the outlet plane. This is likely to result in a reduction of overall mixing but improves the general aerodynamic condition of the flow entering the nozzle guide vanes (NGV).

Further, it was noted that the swirling flow further exacerbated the tendency observed in the previous study for the air flow split between the inner and outer annuli to be biased towards the outer annulus.

Overall though, many negative aspects in the flow of the combustors without swirl were improved such as the removal of cross-sectional vortices and the condition of the outlet plane flow entering the NGV.

2.0 DESIGN PARAMETERS

The Input conditions for the combustor design are given in **Table 1**. The combustor was designed for 5 conditions namely Take off/Max Power, High Altitude Relight, Ground Idle, Flight Idle and Cruise (SL) – Max $\dot{m}_3$. The parameters at each condition were devised using the cycle modelling tool GasTurb [7].

The three design parameters tested (see **Table 2**) were 1) annular area split configuration, 2) Hole area splits and 3) Relative hole positions.

The first aspect varied was the annular area split configuration. Two options were designed:

1. 50/50% area split.
2. 65/35% area split.

This variation resulted in a variation in the inner (d_i) and outer (d_o) combustor liner diameters for the two split ratios.

In order to accommodate a variable annuli air flow split (and associated area split), new liner diameter equations were derived and are show below:

$$d_o = \sqrt{D_o^2 - 0.3x(D_o^2 - D_i^2)} \quad \ldots (\ 1\ )$$

and

$$d_i = \sqrt{D_i^2 + 0.3(1-x)(D_o^2 - D_i^2)} \quad \ldots (\ 2\ )$$

where $x =$ The fraction (out of 1) of total air required in the outer annulus

The second aspect varied was the hole-set configurations and thus annular air flow splits. The following three options were designed:

1. Outer annulus: Pzo, Szo, Dzo, PzV and Inner annulus: Szi, Dzi (65/35% air flow split).
2. Outer annulus: Szo, Dzo, PzV and inner annulus: Pzi, Szi, Dzi (50/50% air flow split).
3. Outer annulus: Pzo, Szo, Dzo and Inner annulus: PzV, Szi, Dzi (50/50% air flow split).

The third aspect varied was the hole configurations of the hole-sets with respect to one another. This aspect required some application of arbitrary rules and logical thought about the aerodynamic consequences of the choices. Considerations included:

1. The available diameters of tubing limited the vaporizer tubes to either 6 or 8 tubes for the prescribed mass flow split. In order to try get more evenly distributed aerodynamic features around the circumference of the combustor the 8-tube configuration was chosen.
2. Each hole-set calculation provides many hole-diameter/number-of-hole configurations. NREC recommends a maximum of 10 holes per hole-set row.
3. This combustor is highly constrained in the lengthwise direction and thus minimising the hole row intrusion into the material in the lengthwise direction was employed as well as attempting to reduce the number of rows per hole-set.
4. The interference (both constructive and destructive) of the hole-sets' flow with each other and the vaporizer tubes was also considered thus various design options were produced where:
    a. Holes could be aligned with the vaporizer tubes or placed in between them to make sure they don't impinge on the vaporizer tubes and their flow isn't disrupted by the vaporizer tubes.

Table 1:
The Input values for the combustor design [8, 9, 10]

Ref. No.	Condition			Compressor outlet data					Turbine inlet data	Combustor				
		Mach No.	alt	p_3	P_3	T_3	$\dot{m}_3$	$\dot{m}_f$	T_4	P_4/P_3 [11]	$\Delta P/P$ [11]	P_4/P_3 [3]	$\Delta P/P$ [3]	Eff
			m	Pa	Pa	K	kg/s	kg/s	K					%
1	**Take off/Max Power**	0	0	425589	425608	501.29	0.35	0.00666	1171	0.94	0.06	0.94	0.06	0.95
2	**High Altitude (relight)**	0.2	2 500	75705	75708	274.08	0.057	0.00149	904	0.97	0.03	0.94	0.06	0.65
3	**Ground Idle**	0	0	123625	123629	309.23	0.08	0.00204	1184	0.98	0.02	0.94	0.06	0.91
4	**Flight Idle**	0.4	2 500	181798	181806	373.99	0.149	0.00209	897	0.96	0.04	0.94	0.06	0.95
5	**Cruise (SL)-max $\dot{m}_3$**	0.6	0	542825	542848	536.14	0.431	0.00756	1153	0.94	0.06	0.94	0.06	0.95

b. The number of holes per hole-set were as designed or modified to various combinations of multiples of the number of vaporizer tubes.

With regards to the primary zone and its recirculation zone, 4 different Pz hole/vaporizer tube configurations were originally tested, however only 2 were used in this study:

1. Vaporizer tube from the outer annulus with Pz holes in outer annulus *in between* the vaporizer tubes (option 1 in **Table 3**)
2. Vaporizer tube from the outer annulus with Pz holes in inner annulus *in line* with the vaporizer tubes (option 2 in **Table 3**)

The two chosen designs for this study covered the design parameter options as follows:

- Design C was of option 1 hole configuration: Annular Area Split = 50/50, Hole area splits (Annular Air Flow Splits) = 65/35
- Design G was of option 2 hole configuration: Annular Area Split = 50/50, Hole area splits (Annular Air Flow Splits) = 50/50

A design comparison between the two combustors is shown in **Table 2** and **Table 3**.

Table 2:
The design choices of the analysed designs.

Design Aspect: →	**Annular Area Split (outer/inner %)**		**Hole-set Configuration & Annular Air Flow Splits (outer/inner %)**		**Hole configurations**
Design No.: ↓	**50/50**	**65/35**	**Option 1 65/35**	**Option 2 50/50**	**Comment**
Design C	✓		✓		• Holes are multiples of vaporizer tubes.
Design G	✓			✓	• Holes are multiples of vaporizer tubes (Pz in line, Sz & Dz offset). • Number of Dz rows further reduced to try decrease lengthwise intrusion but hole sizes kept as designed using NREC momentum flux balancing method.

The compressor diffuser is a tandem blade diffuser with the second row exit plane entering into a "dump diffuser" within the combustor casing section. The second blade row designed exit angle is 35°, thus the theoretical inlet swirl angle indicated from the diffuser blade design of 35° can be seen in **Figure 1**.

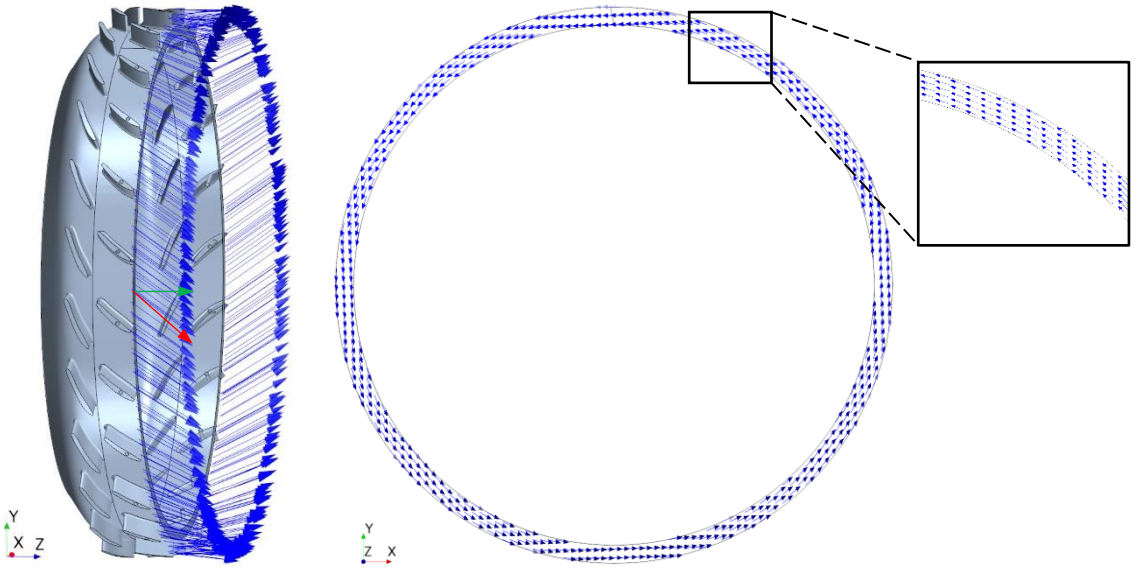

Figure 1: The tandem diffuser blades with the domain inlet swirl at the theoretical blade outlet angle of 35° (blue) in perspective view (left), axial view (right) and close up (inset). A sample vector at 0° (green) and 40° (red) inlet swirl are indicated on the perspective view. $\dot{m}_3$ = 0.35kg/s

Table 3:
A comparison between Design C and Design G

Design C	Design G
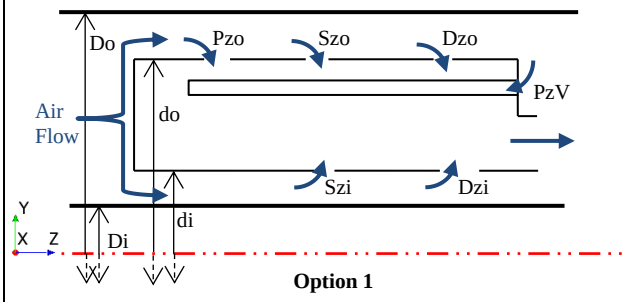	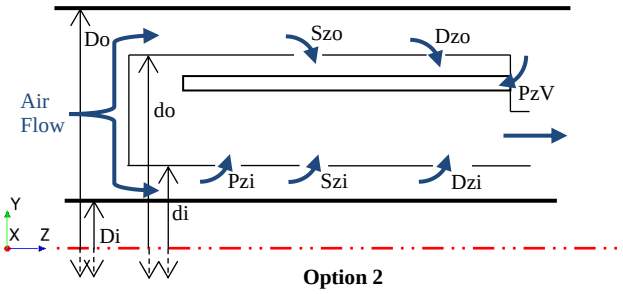
Cross section of the combustor liner showing the hole-set configuration of Design C (Option1) and Design G (Option 2)	
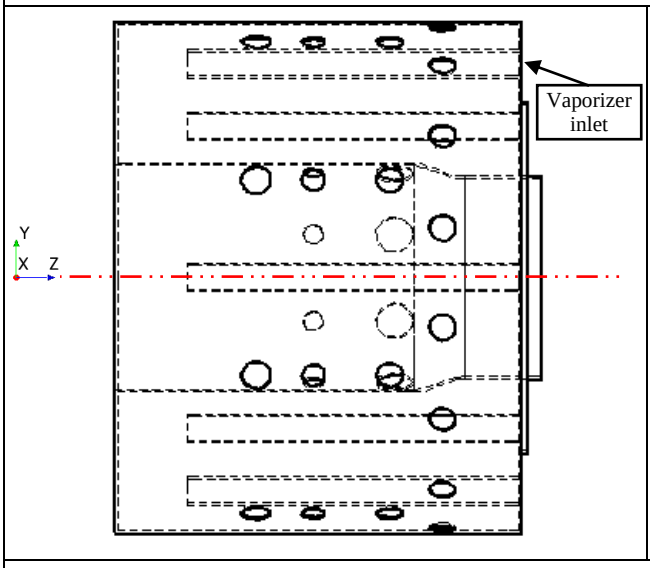	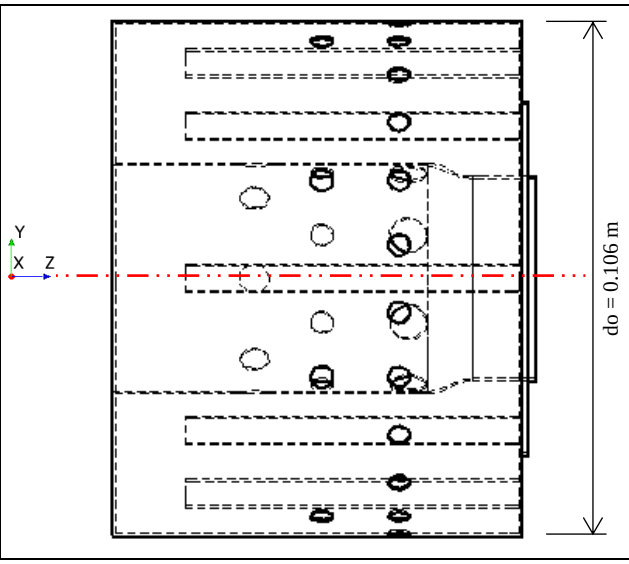
Complete combustor liner geometry showing the hole-set configuration of Design C and Design G	
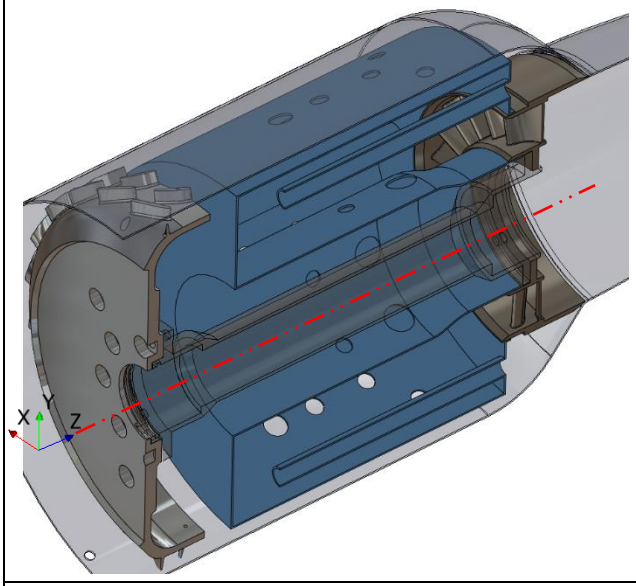	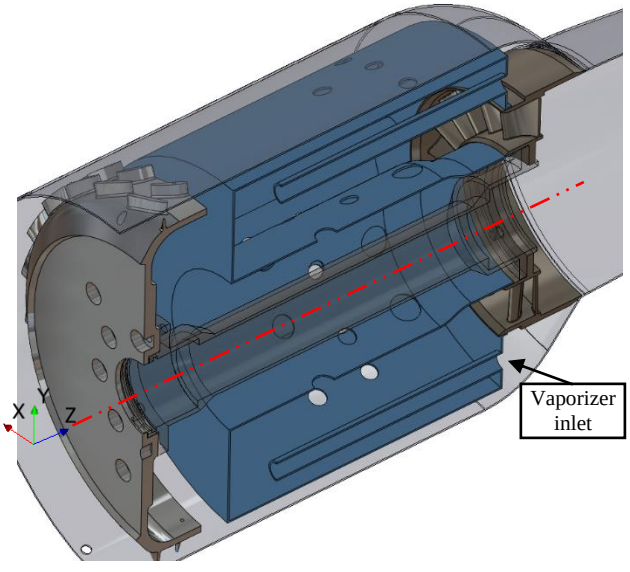
Perspective, cross-sectional view of the installed combustors for Design C and Design G showing the Installed NGV at the combustor outlet	

3.0 METHODOLOGY

3.1 CFD Analysis

In order to investigate the effect of inlet swirl angle on the internal aerodynamics of the previously chosen two combustor designs, the domain inlet flow angle was varied over a range starting at the theoretically ideal case of 0° and straddling the diffuser design angle of 35°. The flow inlet angles tested were 0° (original simulations from [2]), 10°, 20°, 25°, 30°, 33°, 35°, 37°, 40°. A sample inlet boundary condition is shown in **Figure 1** at the 35° inlet angle.

To obtain data comparable to the cold pressure drop used in the NREC preliminary combustor design method [3, 6], no combustion modeling was performed. Cold flow CFD simulations were performed, and the internal aerodynamics of the combustors were evaluated thus giving an indication of the detrimental or advantageous effect of the inlet swirl.

For the RANS CFD modelling, the all-purpose CFD software, STAR-CCM+, was used. The analyses were performed on a simplified model of the combustor where the flow domain excluded the diffuser and NGV sections. The flow domain inlet was placed just downstream of the diffuser and the outlet just upstream of the NGV. Air entered the flow domain at an angle to the boundary in the analyses, dependent on the angle being tested.

Figure 2 shows the model used for the analysis of Design C. The models of both designs were similar, with only the combustor itself changing (green part in **Figure 2**). An initial mesh was developed which consisted of 1036302 mesh cells and later improved through surface refinement, the addition prism cells in the boundary layer regions and local mesh refinement where the holes were located. These changes resulted in a mesh consisting of 4097948 cells but no significant changes in flow patterns were observed. Subsequent simulations were carried out using the mesh settings of the 4 million cell mesh mentioned above.

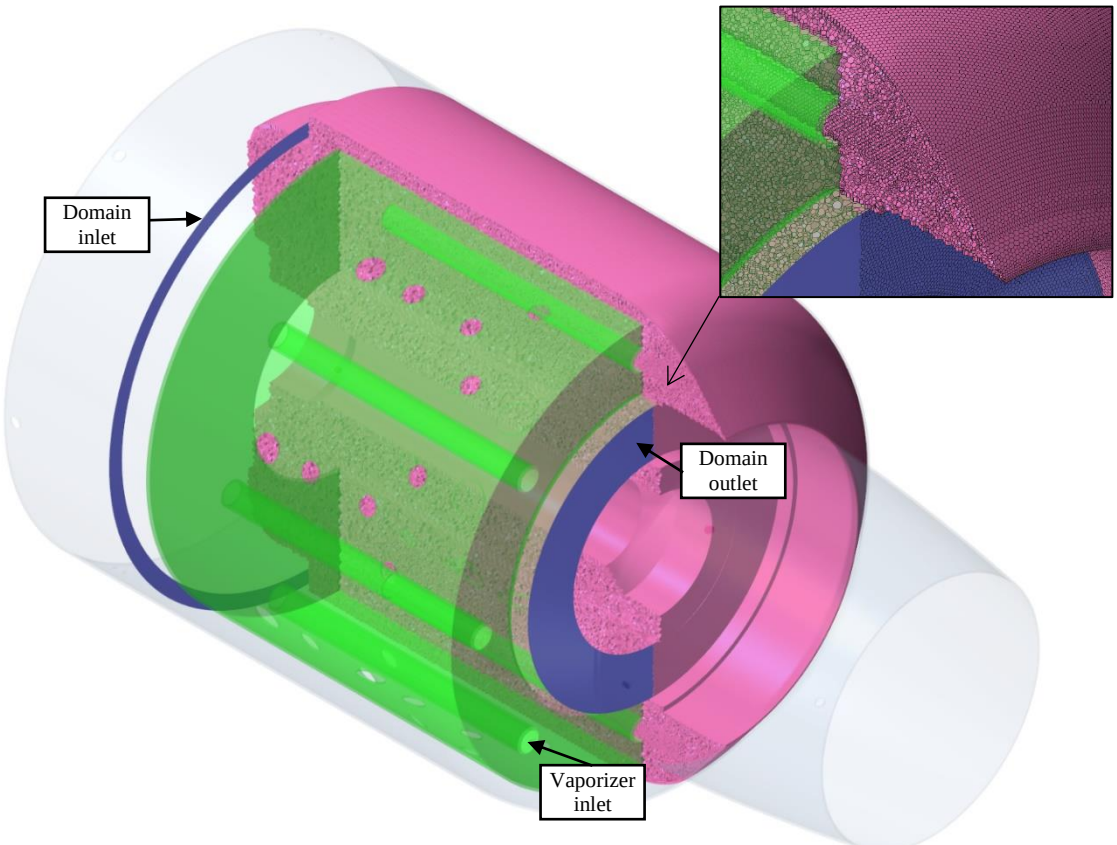

Figure 2: A cross sectional view of the mesh used (pink) with some of the geometry features showing for reference

The boundary conditions corresponding to Condition 1 (Take off/Max Power) in **Table 1** were used. The inlet temperature was specified as 501 K and remained close to that value throughout the domain (see **Figure 3**). The inlet boundary had a pressure specification of 426kPa and an inlet mass flow rate of 0.35kg/s.

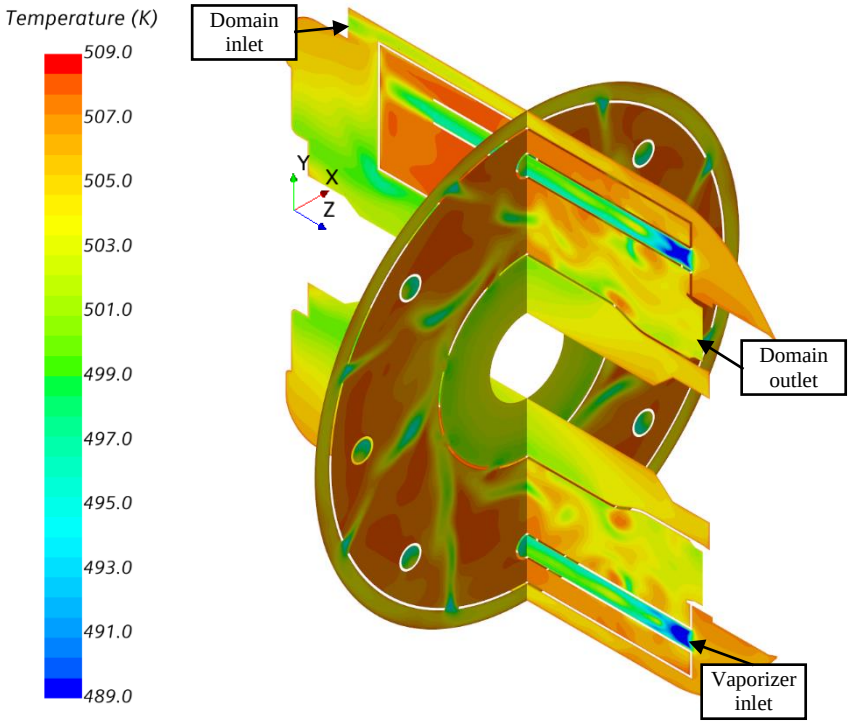

Figure 3: The temperature distribution on representative cross sectional and longitudinal planes for Design C, inlet angle 35°.

The modelling approach was developed and validated in a separate study [12] by comparing results of a CFD analysis of a generic combustor for which experimental data were available [13, 14, 15]. The steady state, k-omega (Menter SST) turbulence model was used.

Due to the unsteady nature of combustor flow, in the validation exercise [12] both the experimental and the CFD data had to be averaged as was the CFD data generated in this study. It was decided to average 100 sets of data, each taken 10 iterations apart from the steady-state solution once it had stabilised. Averaging the results of more than 100 data sets did not improve the accuracy significantly. Typically, 4000 iterations would be performed and then a simulation would be saved for averaging after every 10 iterations up to iteration 5000.

As shown in **Figure 4**, the flow speed was below Mach 0.3 (134.6m/s) almost everywhere in the solution, implying that the segregated flow solver could be used. Simulations were started with the coupled flow solver and the switch to the segregated flow solver was done later. The density specification was left at 'ideal gas' to allow for the adjustment of density using the ideal gas assumption instead of the alternative 'constant density' setting. Using the segregated solver made it possible to use a so-called 'Flow Split' boundary at the outlet, and thus the exit pressure need not be specified and could be calculated.

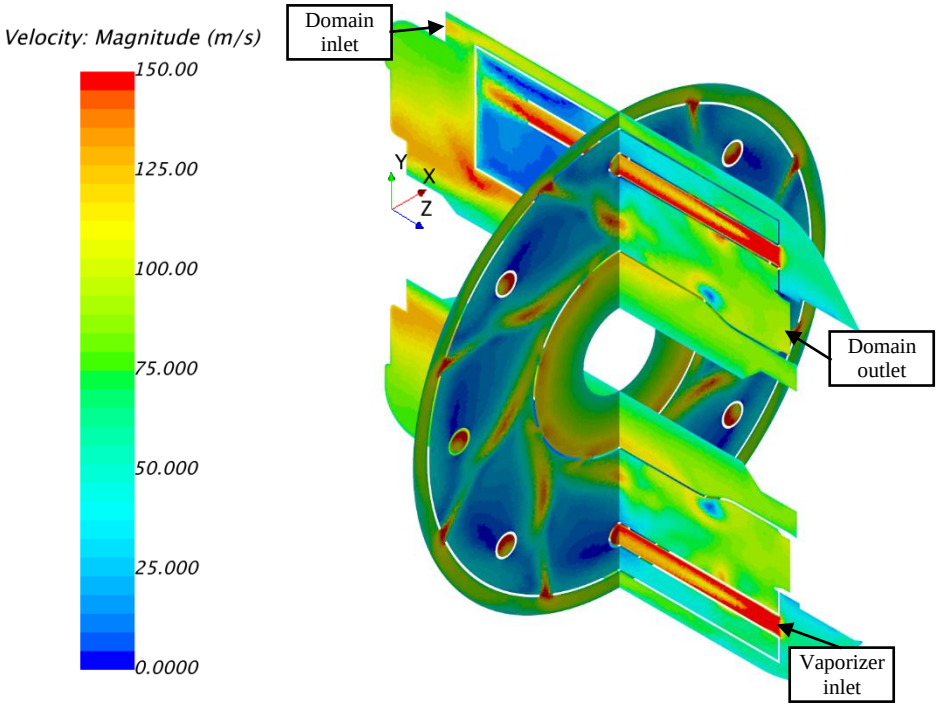

Figure 4: The velocity magnitude distribution on representative cross sectional and longitudinal planes for Design C, inlet angle 35°.

3.2 Scoring and Ranking

The evaluation method used [2] involved the evaluation of the relevant criteria/features, namely, Recirculation zone (Rz), outlet, mixing and pressure drop.

Some of the results such as mass flow split and pressure drop are inherently quantitative, however, the aspects such as the quality of the recirculation zone, mixing and the outlet plane flow are qualitative. In order to apply a more quantitative method for choosing a preferable design, a scoring system was devised in order to apply a quantitative value to the aspects of the flow which are initially analysed subjectively.

In order to analyse the effect of the inlet swirl on the chosen designs, the simulation results were evaluated according to:

- The recirculation zone intensity, shape and position.
- The outlet plane vorticity and the velocity vectors' uniformity and direction.
- The tracer flow paths were evaluated for flow path length and complexity and some interpretation of the mixing might be acquired from these.
- The velocity vector plots were evaluated for the holes' flow interactions, penetrations and influence on the overall combustor mixing through the generation of vortices.
- Combustor pressure drop.

For each feature, the design/swirl combinations were subjectively evaluated relative to each other and given a rating/score.

The mass flowrates and pressure drop are chosen during the design process and thus the values are compared directly (see **Table 4**).

The ideal recirculation zone recirculates combustion gasses back into the Rz from the downstream region to the upstream region. It should also preferably extend in the circumferential direction to allow for as large a region of recirculation as possible. In the case of the longitudinal direction vaporizer tubes, it was also preferable for the

recirculation zone to primarily be positioned towards the inner radial direction rather than squashed in the outer direction between the tube and the outer casing wall.

Ideally, the NGV require straight flow with a uniform velocity distribution from hub to shroud. Based on these requirements, the velocity vectors and vorticity magnitude and components were inspected to determine if there were any vortices or residual swirl at the outlet plane.

The mixing of the combustion gasses with the "cold" flow from the annuli downstream of the primary zone is the mechanism with which the combustion process is meant to be completed as well as the mechanism with which the flow is conditioned for the NGV [6]. The increased mixing in the dilution zone (Dz) serves to condition the temperature distribution (pattern factor) at the outlet. Due to the short length of the combustor, this conditioning is solely due to the mixing from the jets.

Once all of the feature categories were evaluated through the various means (vectors, tracers, vorticity) and a score was given for each design/inlet combination using each evaluation means (see **Table 5**). **Figure 5** to **Figure 18** show sample evaluations of the results showing the best and worst rated representations of each of the 3 major qualitative aspects evaluated. The associated score for each feature is shown.

The next step required the prioritising of the individual feature categories w.r.t. each other and thus an inter-category prioritising and then weighting was applied. The reasoning behind how the weighting was devised is as follows: For a combustor, the Rz is the most important thing to get right and thus has the highest priority. Following that, i.t.o. the engine function, an extremely detrimental outlet plane velocity profile could hinder the engine performance by hindering the turbine functionality. Further, the Mixing contributes to the combustor reaching a more ideal/theoretical functionality while the pressure drop should be minimised, however, increased pressure drop can contribute to the improved functionality of the combustor in the form of increased turbulence intensity and thus improved mixing and functionality. For this reason, a lower pressure drop is desired but not the highest priority due to an advantage to be gained through it. The feature prioritising and weighting are given in the 2nd last and last rows in **Table 5**, respectively.

Once the series of weightings and priorities were applied, the final scores provided a ranking for the design/swirl combinations. This ranking is shown in **Table 6**.

Sample evaluation of the Recirculation zone aspects

Best

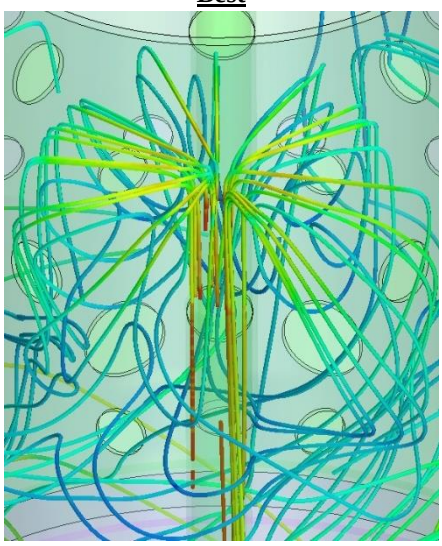

Figure 5: Design G @ 40° - stream tracers showing a fairly good Rz shape. Score 7.5/10

Worst

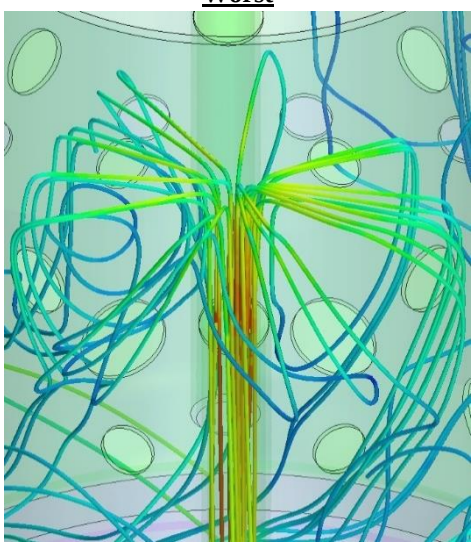

Figure 6: Design G @ 25° - stream tracers showing a bad Rz shape with one side not forming. Score 4/10

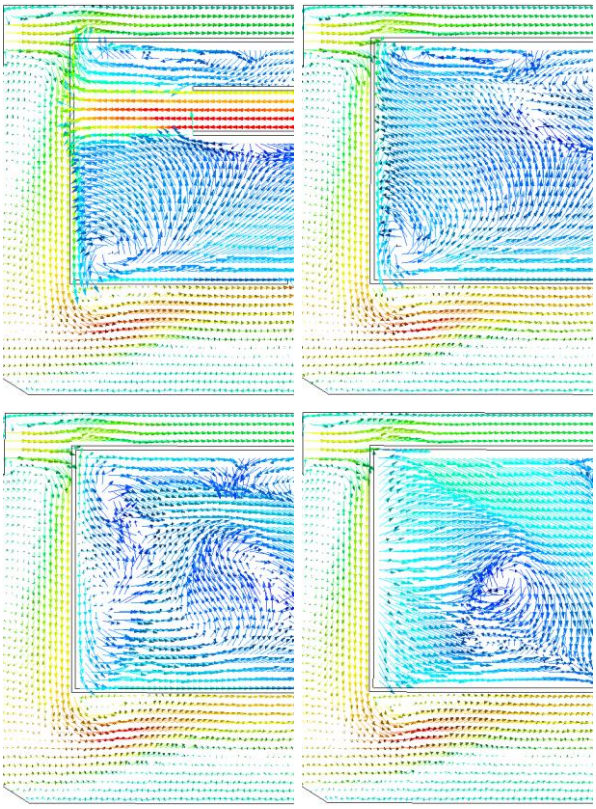

Figure 7: Design G @ 25° - longitudinal C/S vectors showing a fairly good Rz that covers multiple slices. Scored 8.5/10. (slices at 0°, 7.5°, 15°, 22.5° to Y-axis)

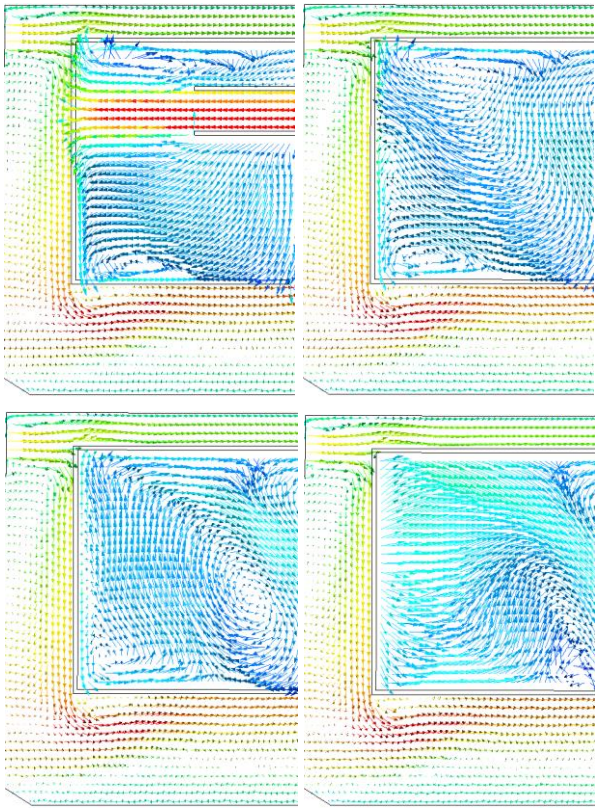

Figure 8: Design G @ 30° - longitudinal C/S vectors showing a Rz that covers only one slice. Scored 3/10. (slices at 0°, 7.5°, 15°, 22.5° to Y-axis)

Sample evaluation of the Outlet plane aspects

Best

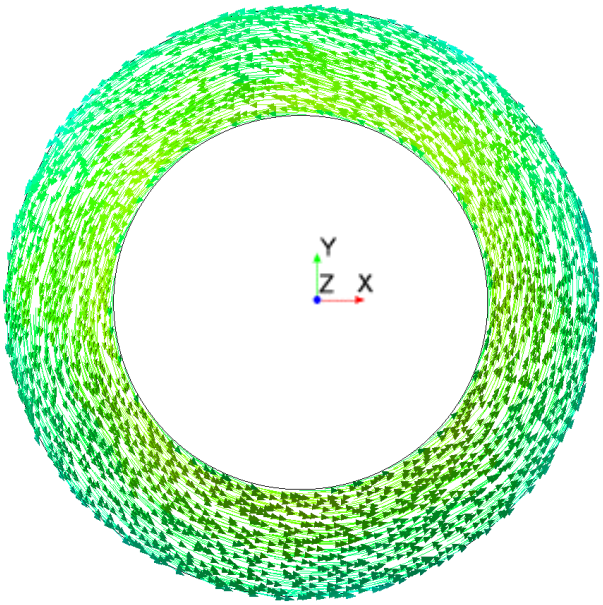

Figure 9: Design C @ 25° - outlet plane velocity vectors showing relatively fewer vortices. Score 6/10

Worst

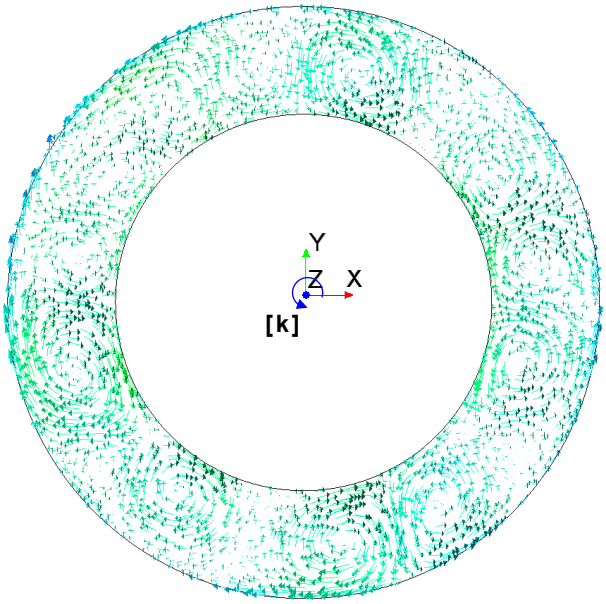

Figure 10: Design G @ 0° - outlet plane velocity vectors showing a large number of vortices. Score 1/10.

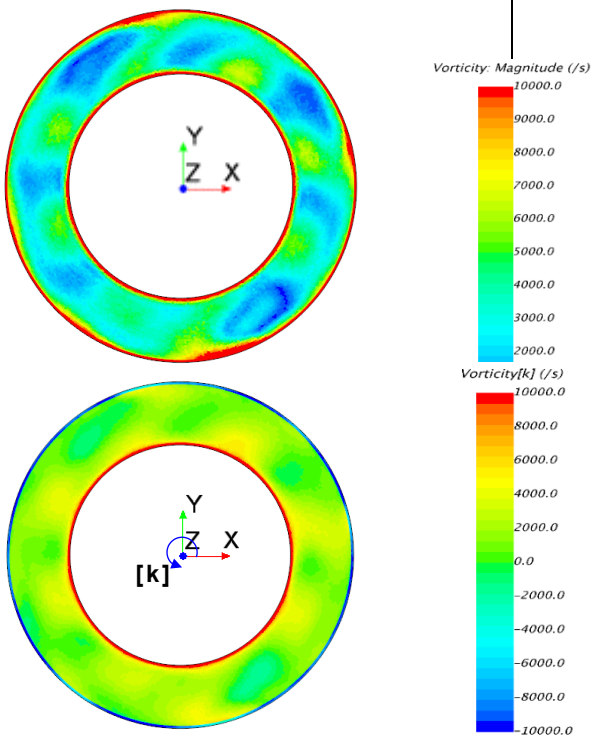

Figure 11: Design C @ 30° - vorticity magnitude (Top) and vorticity about the Z-axis (k unit vector direction) (Bottom) showing a relatively low magnitude and small distribution about the 0 value for the k direction. Score 4/10

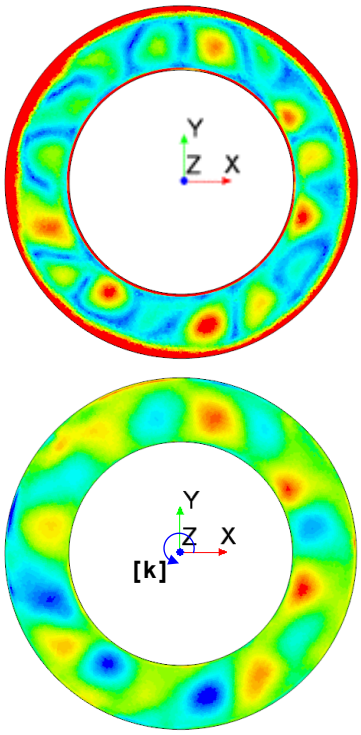

Figure 12: Design G @ 0° - vorticity magnitude (Top) and vorticity about the Z-axis (k unit vector direction) (Bottom) showing a relatively high magnitude and large distribution about the 0 value for the k direction. Score 1.5/10

Sample evaluation of the Mixing aspects

Best

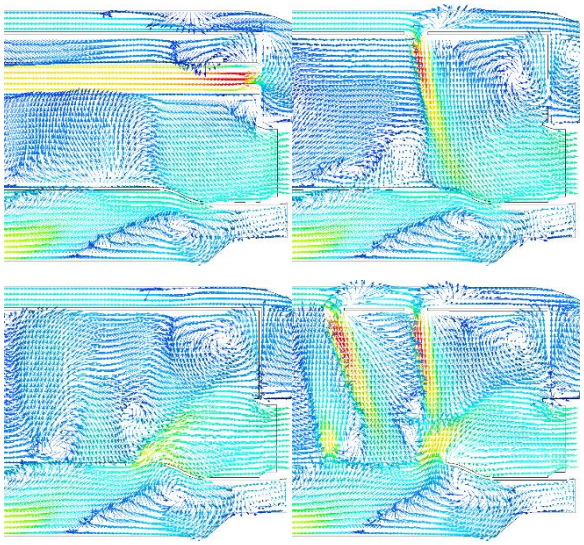

Figure 13: Design G @ 0° - longitudinal C/S vectors showing many, intense vortices in the Sz & Dz. Scored 4.5/10(slices at 0°, 7.5°, 15°, 22.5° to Y-axis)

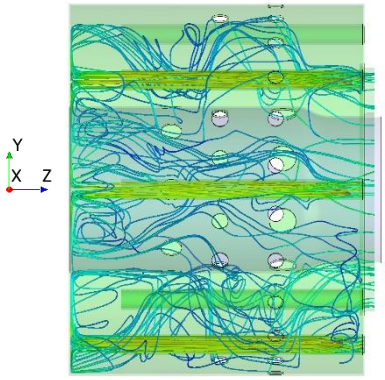

Figure 15: Design G @ 0° - stream tracers showing fairly convoluted tracer paths in the Sz & Dz regions. Score 6/10

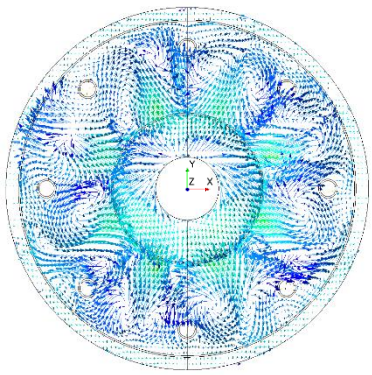

Figure 17: Design G @ 0° - sample C/S velocity plane (after the Sz hole row) showing large, well-formed vortices. Score 5/10.

Worst

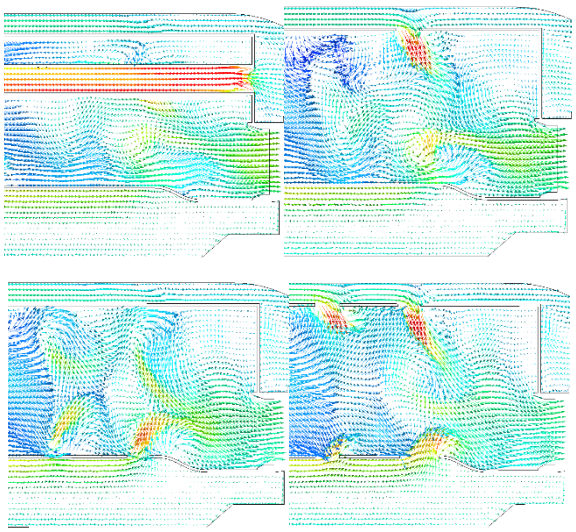

Figure 14: Design G @ 20° - longitudinal C/S vectors showing only a few, weak vortices in the Sz & Dz. Scored 2.5/10. (slices at 0°, 7.5°, 15°, 22.5° to Y-axis)

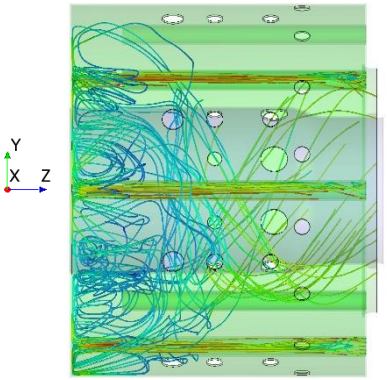

Figure 16: Design C @ 40° - stream tracers showing flow paths that have few direction changes along the length of the Sz & Dz regions. Score 2.5/10

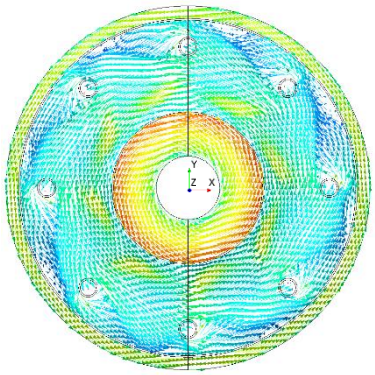

Figure 18: Design G @ 40° - sample C/S velocity plane (after the Sz hole row) showing no vortices. Score 0/10.

4.0 RESULTS AND DISCUSSION

CFD simulations for 18 simulations were performed and the data were processed, analysed and interpreted. These simulations consisted of two different combustor designs, Design C and Design G (see **Table 3**), with 9 different inlet swirl angles being implemented namely 0° (original simulations from [2]), 10°, 20°, 25°, 30°, 33°, 35°, 37°, 40°.

4.1 Quantitative Features

The first step in analysing the data was to evaluate the trends associated with the combustor pressure drops and annuli mass flow splits as the inlet swirl angle was increased. The designed and simulated mass flow splits are shown in **Table 4** and **Figure 19**. The first thing to note is that there is a discrepancy between the Design value and the CFD which can be attributed to a number of factors such as secondary flow effects not being accounted for in the NREC empirical design method. In addition, the combustor is of a much smaller scale than is typically accommodated for in the design method. It can be seen in both Designs C and G that, as the inlet swirl angle increased, the mass flow split to the inner annulus steadily decreased with a corresponding increase of mass flow rate to the outer annulus.

Aside from a deviation in the trend of Design C, inlet angle of 10°, the general trend was for the overall combustor pressure drop to increase from 7.8% to 13.7% and 7.9% to 18.5% for Designs C and G respectively. The original zero swirl designs already exceeded the theoretically designed cold pressure drop of 6%, and this value only gets larger by adding inlet swirl.

Table 4:
The simulated annulus mass flow splits compared to the annulus design parameters

		Design				CFD		
		Area splits %		Mass flow split %		Mass flow split %		Pressure drop
		Outer annulus	Inner annulus	Outer annulus	Inner annulus	Outer annulus	Inner annulus	[%]
Design C	**0°**	50	50	65	35	72	28	7.8
	10°	50	50	65	35	71	29	7.3
	20°	50	50	65	35	74	26	8.2
	22°	50	50	65	35	77	23	9.1
	24°	50	50	65	35	79	21	10.3
	26°	50	50	65	35	81	19	11.2
	30°	50	50	65	35	82	18	11.8
	35°	50	50	65	35	82	18	12.5
	40°	50	50	65	35	84	16	13.7
Design G	**0°**	50	50	50	50	54	46	7.9
	10°	50	50	50	50	55	45	8.0
	20°	50	50	50	50	61	39	10.4
	22°	50	50	50	50	63	37	11.6
	24°	50	50	50	50	66	34	13.4
	26°	50	50	50	50	68	32	14.6
	30°	50	50	50	50	69	31	15.6
	35°	50	50	50	50	70	30	16.7
	40°	50	50	50	50	72	28	18.5

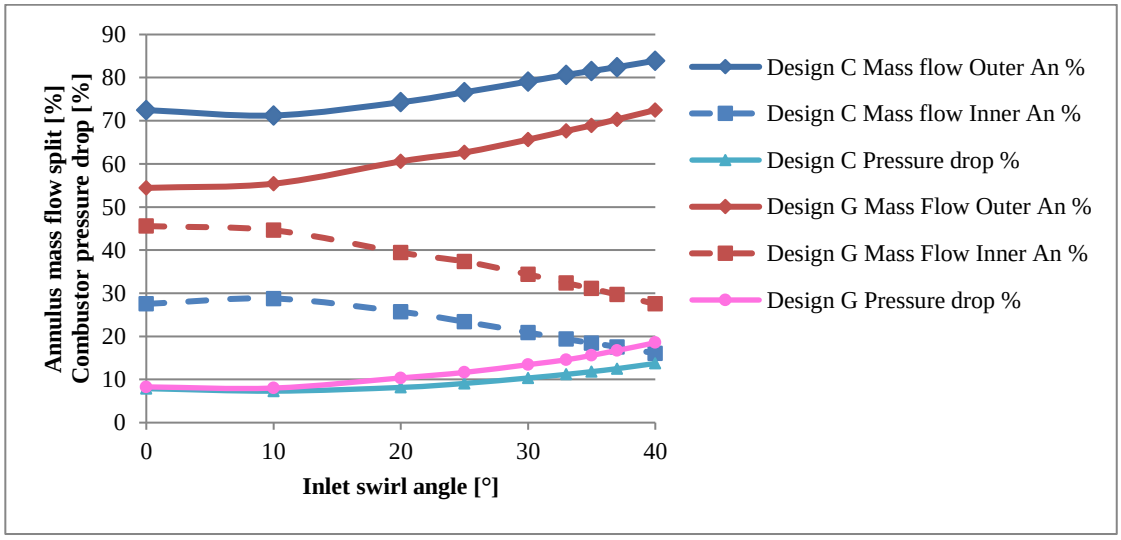

Figure 19: Inner and outer annuli mass flow splits and combustor pressure drop vs inlet swirl angle

4.2 Qualitative features

In order to attempt to apply a more structured approach to evaluating the combustor designs and simulations, the scoring method devised for the choosing of combustor designs [2] (and described in section 3.2) was applied. The individual scores given to each simulation for each output method in each of the 3 categories (Rz, outlet and mixing) are shown in **Table 5**. The general trends and observation for the specific features are discussed below.

Table 5:
The scoring for each simulation for the various feature categories

		pressure drop	Rz (tracers)	Rz (l vectors)	Outlet (vectors)	Outlet (vorticity)	Mixing (l vectors)	Mixing (tracers)	Mixing (C/S vectors)
		[%]	/10	/10	/10	/10	/10	/10	/10
Design C	**0°**	7.8	6.5	7	6	2	4	5	4.7
	10°	7.3	4.5	3	3	2	3.25	5	2.75
	20°	8.2	6	7.5	4	2	3.25	5	0.5
	25°	9.1	6.5	7.5	6	3.5	4.5	4	0.5
	30°	10.3	5	8	6	4	3.75	3.5	0
	33°	11.2	5.25	8	6	4	3.75	3.5	0
	35°	11.8	6.25	8	6	4	3	3	0
	37°	12.5	6.25	7.25	6	4	3	3	0
	40°	13.7	6.5	7.75	6	4	2.75	2.5	0
Design G	**0°**	7.9	6	7.5	1	1.5	4.5	6	5
	10°	8.0	7	7.5	3	3	4	4	2
	20°	10.4	5.5	8	4	1.5	2.5	5	0.5
	25°	11.6	4	8.5	5.5	3	2.5	4.5	0.3
	30°	13.4	5.5	3	6	2	2.75	4	0
	33°	14.6	6.5	8.5	6	2.5	3	3.5	0.3
	35°	15.6	6.5	7.75	6	2	3	3	0
	37°	16.7	6.5	7.5	6	2	2.75	2.5	0
	40°	18.5	7.5	8.25	6	2.5	2.75	2.5	0
Weighting within categories		1	0.75	0.25	0.25	0.75	0.5	0.4	0.1
Feature priority		3	1		2		3		
Feature weighting		1	3		2		1		

For all the simulations, the swirl angle translated into angled flow in both annuli and longer flow paths around the dead ends of the annuli. In general both designs scored fairly well when evaluating the recirculation zones of each simulation. This can be seen in **Figure 20** with the majority of the scores being 5 or above with the scores at the inlet swirl angle of 35° being above 6. The tracer results showed that occasionally some flow that leaves one recirculation zone enters an adjacent one in the direction of the swirl.

Figure 21 shows that the outlet quality improves drastically as the swirl increases when evaluated using the vectors. This is mainly due to the reduction in small swirling vortices exiting the combustor and the co-directional alignment of the flow in a single azimuthal direction around the Z axis. There is also some improvement observed when evaluating the outlet using the vorticity magnitude and components, especially for Design C, however these still indicate some unevenness to the outlet plane.

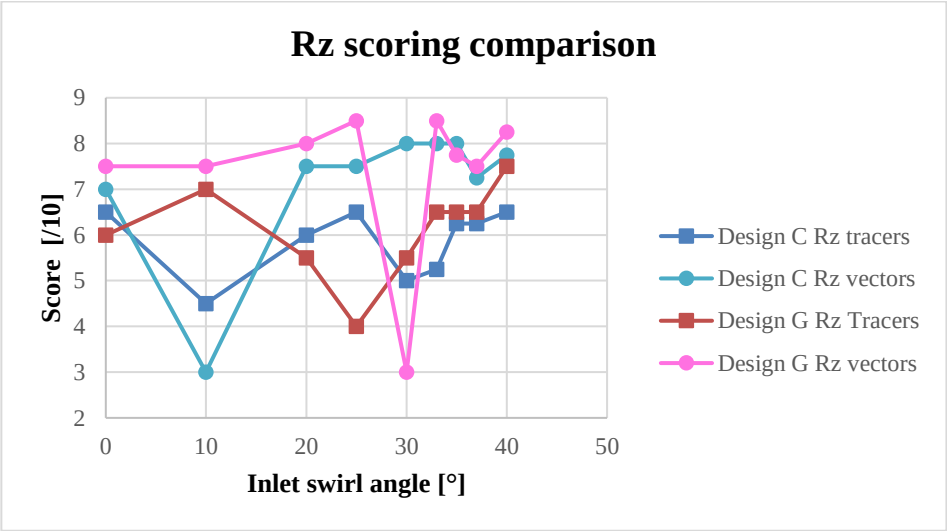

Figure 20: The Recirculation zone scoring for each evaluation method and design vs swirl inlet angle.

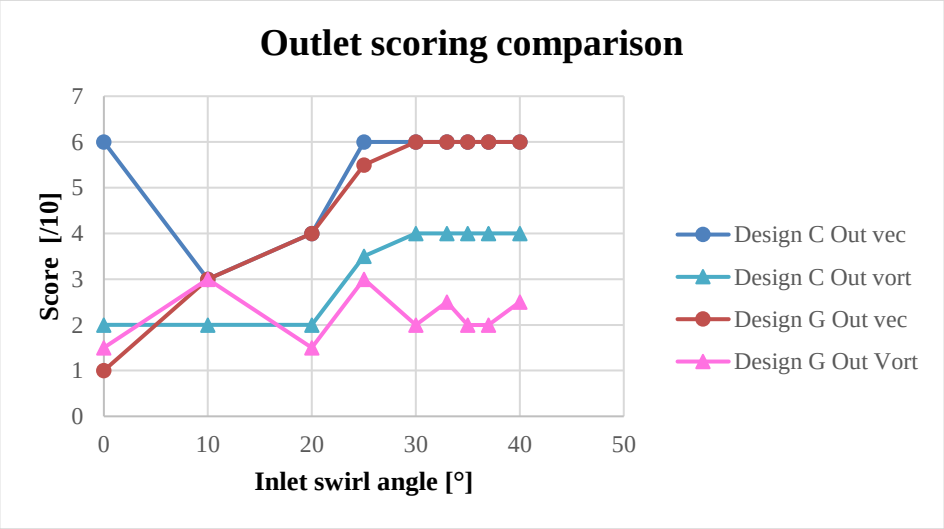

Figure 21: Outlet quality scoring for each evaluation method and design vs swirl inlet angle

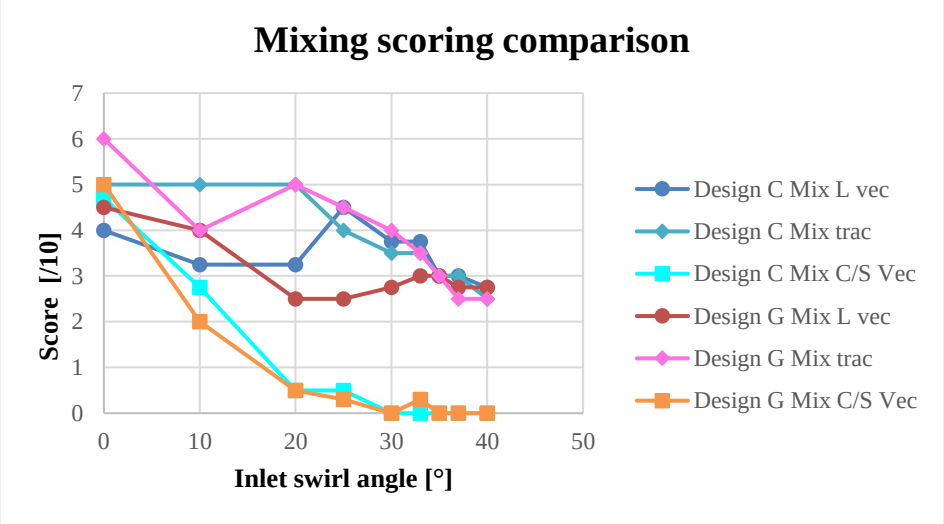

Figure 22: Mixing scoring for each evaluation method and design vs swirl inlet angle

The Mixing scores showed similar trends using all three evaluation methods, longitudinal cross section vectors, tracers and axial cross-sectional slices. There is a general reduction in the score as the swirl angle increased. This behaviour along with the increase in pressure drop, matches the expected behaviour, as indicated by Lefebvre, of an increased pressure drop without necessarily enhancing mixing [6] due to increased swirl. However, there was also a drastic reduction in the vortices in the axial cross-sectional slices. This reduction in the vortices in this direction contributed to the improvement in the scores for the outlet planes since these vortices were not carried downstream to the outlet as in the straight inlet cases. The trends in the different evaluation methods can be seen in **Figure 22**.

After scoring the features using the various evaluation methods, the scores were combined using an intra-category weighting. The weighting for each score is indicated in the 3rd last row of **Table 5**.

The combined score for the recirculation zone evaluation is shown in **Figure 23**. Design C indicates a generally increasing trend in the recirculation zone score from 10° onwards (dashed blue arrow). Design G only has a clear increasing trend after 30° while it had a decrease before that (two dashed red arrows). Despite the slight trends, the scores in general were fairly good except for Design C at 10 degrees. At the diffuser angle of 35°, the two combustor designs fare similarly with scores just below 7.

The inlet swirl was carried through to the outlet plane of the combustor in all cases thus introducing a general swirling to the outlet flow entering the NGV. Swirl in the k direction and about the Z axis can be tolerated by the NGV however swirl in the other 2 directions or in the k direction, but about a different axis, such as can be seen in **Figure 10**, is not well tolerated by the NGV and turbine rotor and can be highly detrimental to the engine performance as any other off axis flows would represent a non-standard design condition for an NGV/turbine blade [16]. As the swirl increased, these vortices seemed to be removed thus the swirl aided in removing the detrimental vortices however it increasingly contributed to non-straight flow entering the NGV. Once the scores are combined for the outlet, a generally increasing trend is observed as the swirl angle increases, as shown in **Figure 24**. Design C has a larger increase than Design G however, the maximum scores flatten out at 4.5. The reason for this is that despite the flow becoming more uniform and exiting at a constant swirl angle, the swirling flow is not ideal for the NGV since they are designed to accommodate flow with zero degree swirl (see **Figure 28**).

Figure 25 shows the combined score of the Mixing evaluation methods and it shows a clear decreasing trend for both combustor designs. Overall there is a decrease in the possible mixing mechanisms within the combustor because the added swirl has a reducing effect on the number and strength of the vortices within the combustor in all directions.

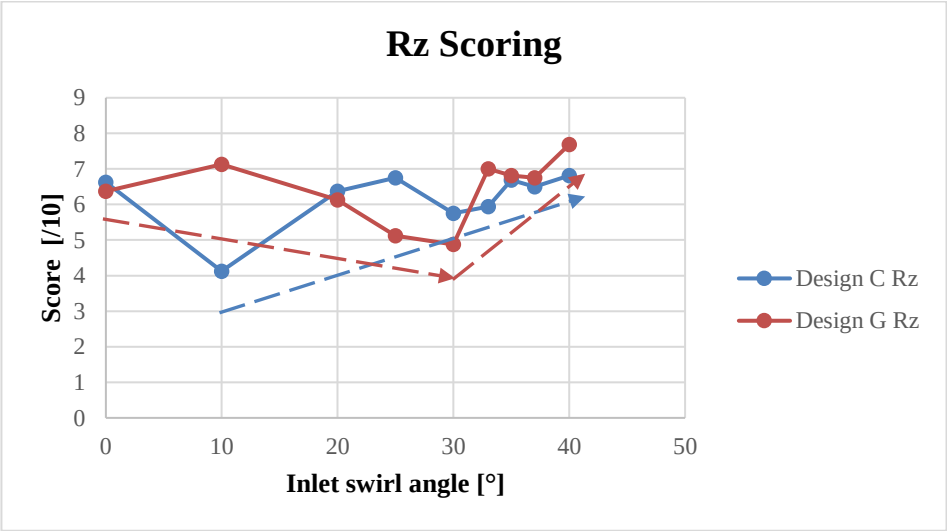

Figure 23: The combined score for the recirculation zone from the various evaluation methods (dashed arrows indicate discussed trends)

Figure 24: The combined score for the outlet from the various evaluation methods

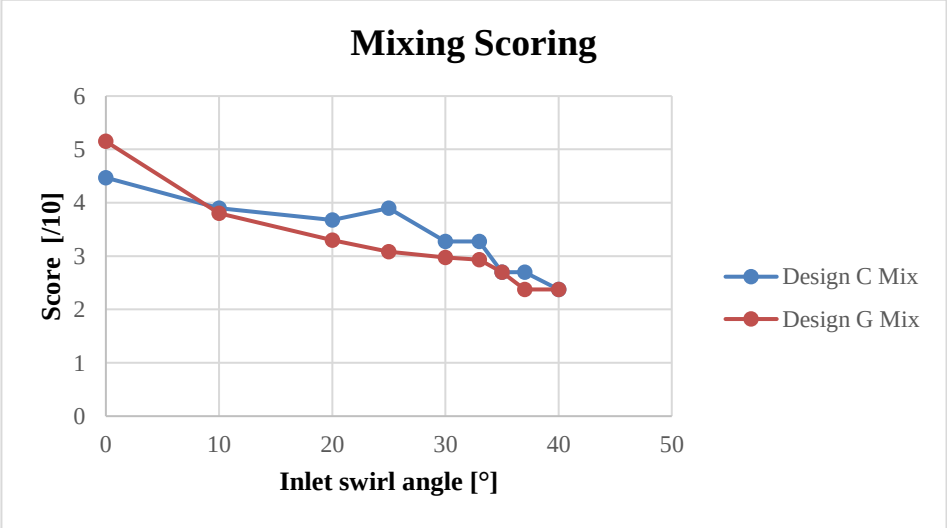

Figure 25: The combined score for the Mixing from the various evaluation methods

In general it can be seen that the scores for mixing and outlet were all fairly low and not as high as one might want, however, this could be expected due to the first hole-set design phase focusing on the improvement of the Rz and the study to improve the Sz and Dz not yet performed.

After applying the Feature weightings as shown in the last row of **Table 5** and calculating the final scores for the current set of simulations, the simulations were ranked as shown in **Table 6** and **Figure 26**. A slight increasing trend can be seen for Design C in **Figure 26** which is not the case for Design G. This indicates that Design C is able to tolerate a greater range of swirl angles with likely adequate performance, as might be the case with varying mass flow rate changes through the various engine operating points. It can also be seen from **Table 6** that, except for 10° and 33°, Design C always scores higher than Design G for all angles.

At the 35°inlet swirl condition which correlates to the engine diffuser design angle of 35°, Design C too scores higher than Design G which biases the design choice for this engine further to Design C when including the effect of inlet swirl in the design choice considerations.

Table 6:
The scoring for each simulation for the various feature categories

Ranking	Design	Inlet swirl angle	Final Score [%]
1	Design G	10°	76
2	Design C	25°	74
3	Design C	0°	65
4	Design C	40°	64
5	Design G	33°	64
6	Design C	35°	63
7	Design G	40°	60
8	Design C	30°	56
9	Design C	33°	55
10	Design C	37°	55
11	Design G	35°	48
12	Design C	20°	47
13	Design G	0°	45
14	Design G	25°	40
15	Design G	37°	40
16	Design G	20°	36
17	Design C	10°	34
18	Design G	30°	27

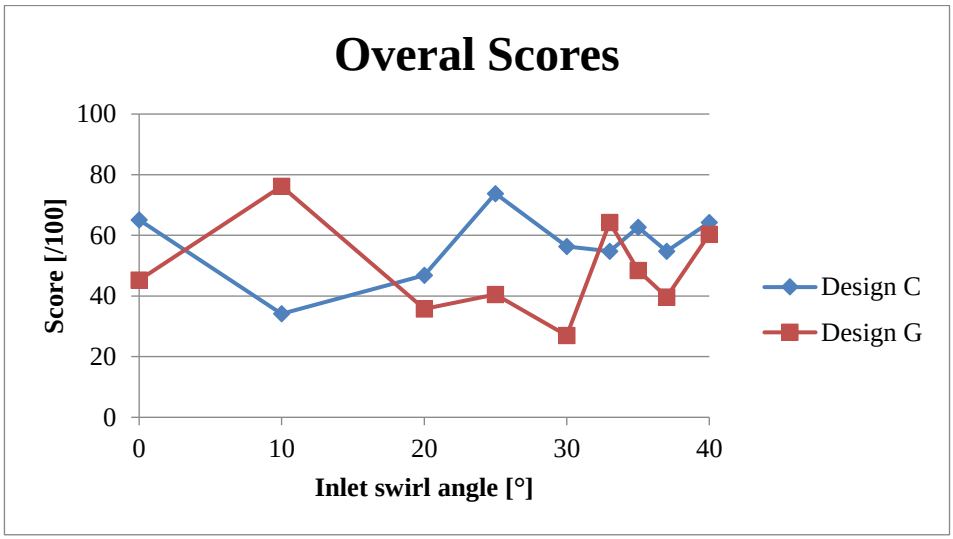

Figure 26: The trend of the scores per combustor design as the inlet swirl angle is increased

In addition, the rankings were recalculated in the global context where the data subset from the previous study [2] were included in the ranking with the current inlet swirl study data subset. These results are shown in **Table 7**. In this table it can be seen that despite the increased inlet swirl reducing the scores of the chosen two designs C and G, they are still generally better than designs A, B and F while Design C fell in the top half of the ranking for a majority of the swirl angles.

For the Global context ranking, however, an anomaly has become apparent where the orders of the two data subsets are not necessarily maintained when combined. This suggests two aspects for further investigation:

- The method to evaluate the data might need to be adjusted
- This potentially warrants a future detailed analysis of some other designs such as Design D, E or I

However, for each of the data subset analyses, a check was performed to determine that the ranking outcome correlates with the original scoring assigned to each parameter and the design's overall placement. The current scoring method passed the check in the straight combustor set (i.e. choosing a design) [2] as well as for using the method for checking the effect of swirl on a particular design in this current study.

Table 7:
The final ranking and scores for the simulations tested in the global context

Rank	Simulation		
	Design	**Inlet swirl angle**	**Score [%]**
1	Design G	10°	77
2	Design C	25°	71
3	Design C	0°	68
4	Design I	0°	64
5	Design G	33°	63
6	Design C	40°	63
7	Design G	40°	62
8	Design C	35°	62
9	Design E	0°	62
10	Design D	0°	58
11	Design C	37°	56
12	Design C	30°	55
13	Design C	33°	54
14	Design G	0°	53
15	Design C	20°	52
16	Design G	35°	50
17	Design H	0°	47
18	Design G	37°	44
19	Design G	20°	41
20	Design G	25°	41
21	Design C	10°	38
22	Design A	0°	33
23	Design B	0°	32
24	Design G	30°	30
25	Design F	0°	23

4.3 Outlet properties

One of the features that was affected the most due to the addition of inlet swirl was the outlet plane quality which showed a large improvement, however, the scores were limited to 4.5 as can be seen in **Figure 24**. This lower scoring is primarily due to the NGV being designed for the ideal, straight, incoming flow (see **Figure 28**) while the flow from the combustors is swirling.

It was noted that the swirl entering the combustor is not only maintained but increased throughout the length of the combustor and thus a single directional swirling flow is dominant at the outlet plane. This can be seen in **Table 8** and **Figure 27** with there being an increase in the swirl angle at the outlet up until a ratio of about 1.3 at the higher angles.

Based on this result, the outlet swirl could allow for the negating of NGV before the turbine since the flow is fairly well conditioned and “pre-turned” due to the inlet flow swirling progressing to the outlet of the combustor. The removal of the traditional NGV allows for a reduction in NGV pressure losses which compensates for the increased

combustor pressure loss experienced due to increased inlet swirl. For this engine, the pressure losses in the NGV are 11.16% of the NGV inlet pressure as calculated using Kacker and Okapuu's [17] modification to Ainley and Mathieson [18] methods as implemented by Aungier [19].

Table 8:
A comparison between the inlet an outlet swirl angles for the various designs.

	Inlet angle	Outlet angle	Difference	Ratio
Design C	0	7.1	7.1	-
Design C	10	22.6	12.6	2.260
Design C	20	35.3	15.3	1.766
Design C	25	41.1	16.1	1.644
Design C	30	47.4	17.4	1.580
Design C	33	49.7	16.7	1.508
Design C	35	50.8	15.8	1.452
Design C	37	51.4	14.4	1.389
Design C	40	52.3	12.3	1.308
Design G	0	9.3	9.3	-
Design G	10	20.4	10.4	2.039
Design G	20	35.3	15.3	1.764
Design G	25	41.7	16.7	1.668
Design G	30	45.9	15.9	1.531
Design G	33	47.2	14.2	1.431
Design G	35	48.4	13.4	1.383
Design G	37	49.9	12.9	1.348
Design G	40	51.6	11.6	1.290

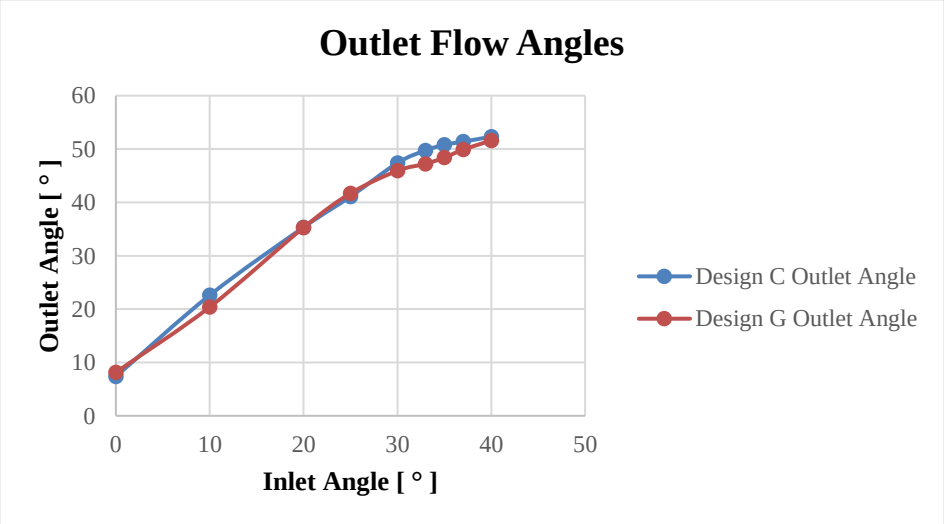

Figure 27: The inlet and outlet flow angles for the various designs

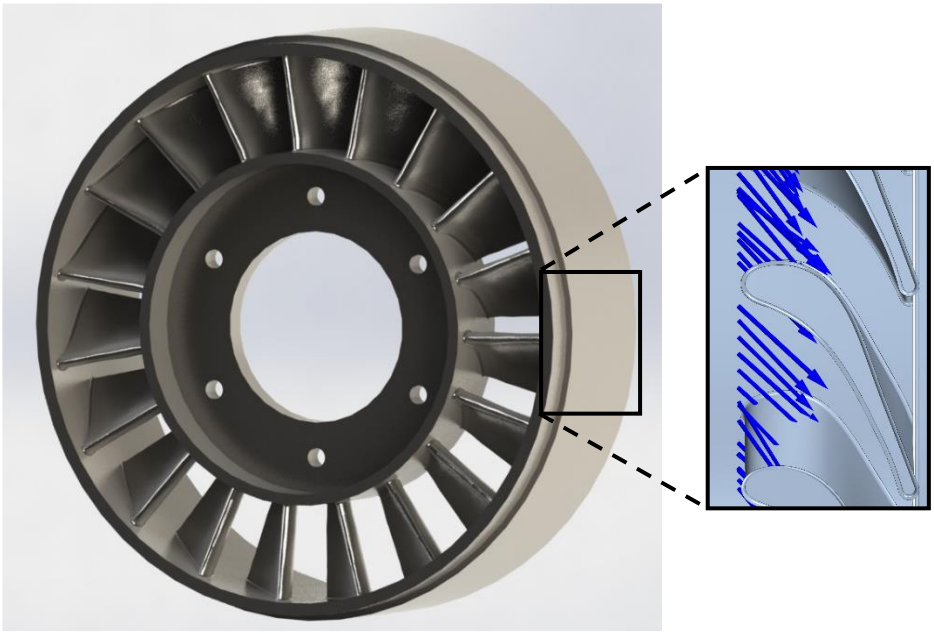

Figure 28: Turbine Nozzle Guide Vanes in perspective view (left) and cut-out side-view closeup with outlet vectors from the 35° inlet swirl analysis and the NGV Leading edge comparison (right).

5.0 CONCLUSION

The 200N combustor was used as a test subject to evaluate the effect of swirl in the flow at the combustor inlet.

The results indicate that increasing inlet swirl has a generally reducing effect on the generation of vortices throughout the combustor liner with a higher influence in the reduction of the vortices generated on the cross-sectional planes of the combustor. This is likely to result in a reduction of overall mixing within the combustor liner. This reduction in cross-sectional vortices, however, reduces the number of vortices at the combustor outlet and thus, improves the general condition of the flow entering the NGV. In addition, the swirl entering the combustor is increased throughout the length of the combustor, as a result of the conservation of angular momentum, and thus a single directional swirling flow is dominant at the outlet plane. This feature could indicate that it could be possible to remove the NGV from this particular small engine design since the turning of the flow, typically performed by the NGV, is already achieved at the combustor outlet. This could reduce the losses by the 11.16% experienced in the NGV which would compensate for the increased combustor pressure loss experienced due to increased inlet swirl. This configuration should be the subject of further investigation.

Design C generally performed better than Design G with the addition of swirl when combining the effects of the different features.

Further, it was noted that the swirling flow further exacerbated the tendency observed in the previous study for the air flow split between the inner and outer annuli to be biased towards the outer annulus. The advantage of this, combined with the swirling component of the flow, was a reduction in the tendency for the inner annulus flow to have fluctuating vortices at the end which in turn stabilised the flow entering the holes of the inner annulus.

Overall though, some negative aspects in the flow of the combustors without swirl were improved, such as the removal of cross sectional vortices and the condition of the outlet plane flow entering the NGV.

Further, when comparing the two designs' performance at the diffuser design exit angle of 35°, with regards to each of the relevant aspects/features, the Design C and Design G

performances were very similar except for the behaviour at the outlet where Design C scored significantly higher than Design G.

In addition, the scoring methodology for ranking different combustor designs proved to be an effective method to evaluate the effect of inlet swirl on the flow features and behaviour of a particular combustor design, however, an investigation into the ranking behaviour in a multi-data global context application should be the subject of further studies. Using CFD and the ranking system allows for the determining of the effect of various parameters and allows for the testing of certain design choices. This in turn provides an indication of the likely performance changes to be expected and allows for a more informed choice when applying design modifications and interactions during the Preliminary combustor design phase.

Overall, in this case, there seems to be the potential for improvement in the combustor performance with the inclusion of inlet swirl to the combustor.

ACKNOWLEDGMENTS

This document is the result of a research effort funded by Armscor in terms of Order KT471101.

REFERENCES

[1] B. C. Meyers, “The Preliminary Design of an Annular Combustor for a Mini Gas Turbine,” in *Proceedings of the XXII ISABE Conference*, Phoenix, USA, 25-30th October, 2015.

[2] B. C. Meyers and J.-H. Grobler, “The Numerical Aerodynamic Evaluation of Geometrical Configurations of a Vaporizer Tube Micro-Gas Turbine Combustor,” in *Proceedings of the XXIV ISABE Conference*, Canberra, Australia, 22-27th September, 2019.

[3] Northern Research and Engineering Corporation, The Design and Development of Gas Turbine Combustors; Volume II; Design Methods and Development Techniques, Woburn, Massachusetts: Northern Research and Engineering Corporation, 1980.

[4] C. Delord, P. Gauthier, G. Snedden, C. Celis, V. Sethi and P. Pilidis, “Numerical Study of Fuel Atomisation and Vaporisation in a Micro Turbojet Vaporiser Tube,” in *Proceedings of the XXIII International Symposium on Air Breathing Engines (ISABE)*, Manchester, United Kingdom, 3-8 September 2017.

[5] Northern Research and Engineering Corporation, The Design and Development of Gas Turbine Combustors; Volume I; Component Theory and Practice, Woburn , Massachusetts: Northern Research and Engineering Corporation, 1980.

[6] A. H. Lefebvre and D. R. Ballal, Gas Turbine Combustion: Alternative Fuels and Emissions, 3rd ed., Taylor and Francic Group, 2010.

[7] J. Kurzke, *GasTurb v12,* 2013.

[8] J. D. Mattingly, W. H. Heiser and D. T. Pratt, Aircraft Engine Design, 2nd Edition ed., J. S. Przemieniecki, Ed., Reston: American Institute of Aeronautics andAstronautics, 2002.

[9] R. K. Mishra, “Altitude Relight Characteristics of an Aero Gas Turbine Combustor,” in *Seventh National Conference on Air Breathing Engiens and Aerospace Propulsion*, Kanpur, 5-7 November 2004.

[10] R. W. Read, “Experimental Investigations into High-Altitude Relight of a Gas Turbine,” 2008.

[11] P. P. Walsh and P. Fletcher, Gas Turbine Performance, 2nd ed., Blackwell Science Ltd, 1998, 2004.

[12] D. I. Dunn, B. C. Meyers, G. C. Snedden, J.-H. Grobler, R. Moodley and P. Rossouw, “Engine Technology: Engine Systems Evaluation,” Council for Scientific and Industrial Research, Doc. No.: ASC-CHEV-19-0001 RPT, February 2019.

[13] B. C. Meyers, G. C. Snedden, J. P. Meyer, T. H. Roos and G. I. Mahmood, “Three-component particle image velocimetry in a generic can-type gas turbine combustor,” *Proceedings of the Institution of Mechanical Engineers, Part A: Journal of Power and Energy*, vol. 226, no. 7, pp. 892 - 906, 2012.

[14] B. C. Meyers, G. C. Snedden, J. P. Meyer, T. H. Roos and G. I. Mahmood, "Experimental Results Showing the Internal Three-Component Velocity Field and Outlet Temperature Contours for a Model Gas Turbine Combustor," in *20th ISABE Conference*, Göteborg, Sweden, September 12-16, 2011.

[15] B. C. Meyers, "The experimental flowfield and thermal measurements in an experimental can-type gas turbine combustor," University of Pretoria, 2009.

[16] H. Saravanamuttoo, G. Rogers and H. Cohen, Gas Turbine Theory, 5th ed., Pearson Education Limited, 2001.

[17] S. C. Kacker and U. Okapuu, "A Mean Line Prediction Method for Axial Flow Turbine Efficiency," *ASME. J. Eng. Power,* vol. 104, no. 1, pp. 111 - 119, January 1982.

[18] D. G. Ainley and G. C. R. Mathieson, "A Method of Performance Estimation for Axial-Flow Turbines," Aeronautical Research Council, London, 1951.

[19] R. H. Aungier, Turbine Aerodynamics: Axial-Flow and Radial-Inflow Turbine Design and Analysis, New York: ASME Press, 2005.